Periodica Polytechnica Electrical Engineering and Computer Science, 67(2), pp. 194–203, 2023

Investigation on Losses with Various Emerging Core and Winding Materials in a High Frequency Planar Transformer

Arya Venugopal[1], Femi Robert[1*]

[1] Department of Electrical and Electronics Engineering, College of Engineering and Technology, SRM Institute of Science and Technology, SRM Nagar, Potheri, Kattankulathur, 603203 Chennai, Tamil Nadu, India
[*] Corresponding author, e-mail: femir@srmist.edu.in

Received: 25 August 2022, Accepted: 02 December 2022, Published online: 31 January 2023

Abstract

In this work, various emerging core and winding materials suitable for a high frequency planar transformer (PT) has been analyzed and compared. Core and winding materials used in a transformer has a significant effect mostly in the core and winding losses of the transformer. Emerging core materials like amorphous and nanocrystalline cores were compared against the conventional ferrite core. The results obtained showed that core losses were reduced by around 48.14% on using amorphous or nanocrystalline cores instead of the conventional ferrite cores. Typical copper and aluminum windings were also compared with emerging materials like carbon nanotube (CNT), Cu/CNT and Al/CNT. Winding losses was found to be the lowest on using CNT windings instead of metal windings like Cu or Al, or metals composite windings like Cu/CNT and Al/CNT. A winding loss reduction of about 56.2% was seen with CNT windings. Thus, it was concluded that the best possible core and winding combination was amorphous or nanocrystalline cores with CNT windings, as they give the lowest possible core and winding losses for the PT. Finite Element Analysis was carried out on a 2-kW PT operating at 100 kHz frequency, with the software Altair FLUX for the analysis.

Keywords

materials, planar transformer, losses, amorphous, nanocrystalline, carbon nanotube

1 Introduction

Planar transformer (PT) is an emerging power electronic technology that uses planar primary and secondary windings for a high frequency operating transformer [1]. The main advantage of high frequency operating transformers is the smaller profile design obtained for any given power rating [2]. Thus, a higher power density is also seen for these transformers. But there are associated challenges of increased core and copper losses with these high frequency transformer designs, due to phenomena like skin and proximity effects, fringing losses etc. In a PT, instead of traditional helical wire windings around the core, planar windings are arranged on flat Printed Circuit Boards (PCBs). So, winding losses of the transformer will be reduced as the current distribution on the windings is more uniform with the planar winding arrangement, which will also help in reducing skin and proximity effects. The core losses in transformers operating at high frequency are mainly due to non-uniform magnetic flux density distribution. Better performance is seen when the transformer operates closer to it its saturation magnetic flux density value of the core [3]. Stray magnetic flux lines developed in the gaps of the transformer core causes fringing losses in the PT [4]. Such undesired gaps in the core are significantly reduced due to the stacked arrangement of windings, PCB layers and insulators in a PT structure [5].

Selection of appropriate material for core and winding is hugely important in improving the efficiency and reducing the losses of a PT. Many advanced soft magnetic materials like amorphous and nanocrystalline materials [6] are emerging these days to replace the conventional ferrite core of high frequency transformers. Alternatives for ferrite have been introduced as ferrites have very low magnetic flux density. Magnetic flux density values of typical ferrites vary from about 0.3–0.5 T, whereas the emerging amorphous and nanocrystalline materials have magnetic flux density values of more than 1 T [7]. Hence, they have a wider range of applications, along with reduced core loss values due to their thin foil and ribbon-like structures [8]. Carbon nanotube (CNT) and its composites [9] are the state-of-the-art materials introduced to

Cite this article as: Venugopal, A., Robert, F. "Investigation on Losses with Various Emerging Core and Winding Materials in a High Frequency Planar Transformer", Periodica Polytechnica Electrical Engineering and Computer Science, 67(2), pp. 194–203, 2023. https://doi.org/10.3311/PPee.21054

replace the conventional copper and aluminum windings used in transformers [10]. CNT materials have a significantly lower density [11] than metal conductors like copper and aluminum, thereby helping in reducing the overall size of the transformer. They are more stable at higher frequencies and temperatures [12], making them a better choice for high frequency operating transformers like PTs. To improve the conductivity of pure CNT for its usage as an electrical winding material, composites of CNTs are introduced [13, 14], which are made by infusing metals like copper and aluminum into CNT, which gave rise to Cu/CNT and Al/CNT materials respectively.

In most traditional wire-wound transformer optimization problems [15], lifetime costs of the transformers including running and cooling costs are also considered in addition to performance optimization. But in the case of planar transformers, these additional cooling and running costs are not significant due to the permanent planar winding arrangement with inbuilt heat sinks and unvarying PCB currents. Thus, this work is focused only on minimization of losses and thereby optimizing of the transformer performance. In this work, Finite Element Modelling (FEM) was used to study the core and windings losses, weight and efficiencies of a PT with various materials. Analysis and comparison of various core and winding materials suitable for a high frequency, medium power PT has been done, to determine the combination of core and winding material that gives the least possible losses for a PT. Amorphous and nanocrystalline core materials were compared against the conventional ferrite core, and typical copper and aluminum windings were also compared with emerging materials like CNT, Cu/CNT and Al/CNT. Also, efficiency of conventional ferrite core with copper windings was compared with nanocrystalline core and CNT windings, to determine the improvement in efficiency. This paper is divided into the following sections: Section 2 gives the structure and modelling of the PT, Section 3 gives a brief account of the various core and winding materials used for analysis, Section 4 gives the estimation of core losses of the PT with various materials, Section 5 gives the estimation of winding losses of the PT with various materials, and finally Section 6 gives a conclusion of the work.

2 Structure and modelling of the PT

The basic structure of the PT modelled in the simulations is shown in Fig. 1.

A basic EE core is designed with its various layers of windings, PCBs and insulators arranged in a stack within

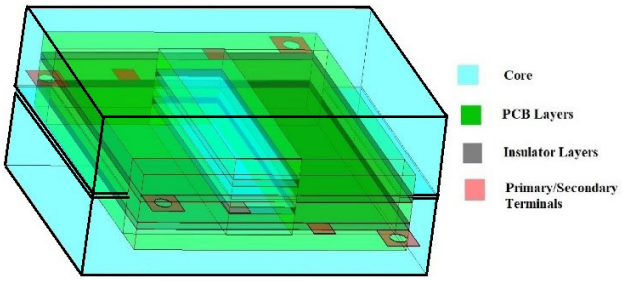

Fig. 1 Structure of the PT

two window areas of the core. A very small air gap of 0.1 mm is maintained between the two E halves of the core. Fringing losses accompanied with air gaps is minimized by ensuring such a small air gap [16]. The stacking arrangement of layers employed in this design is as follows: a top-most layer of PCB carrying one half of the primary winding, an insulator strip, followed by a second layer of PCB carrying one half of the secondary winding on one side, and another half of the secondary winding on the other side, followed by another insulator strip, and finally, a third layer of PCB carrying the second half of the primary winding. The winding arrangement used for the design is shown in Fig. 2.

An interleaved winding arrangement is employed with alternate primary and secondary windings, that is, without a continuous stretch of any one of the winding. Thus, the inter-winding and intra-winding parasitic effects like leakage inductance and stray capacitance are significantly reduced with this winding arrangement [17]. Also, two terminals each are extended out from each of the four windings for connecting the inputs and the outputs.

Transformer impedance minimization is important in reducing transformer losses. In conventional wire-wound transformers, short circuit problem is a potential challenge in impedance minimization. Whereas in planar transformers, since the windings are etched on PCBs, a defined inductance and thereby a reduced impedance is obtained with a lumped design. In this paper, an interleaved winding design as shown in Fig. 2 is employed, which further ensures elimination of short circuit problems, and helps in increasing the efficiency and life of the transformer.

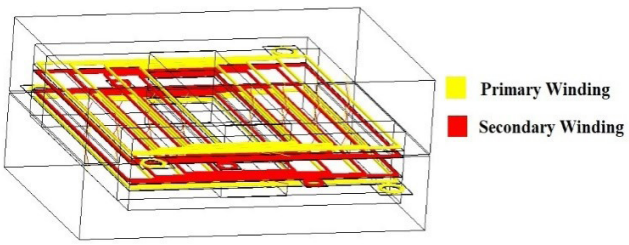

Fig. 2 Winding arrangement of the PT

Major specifications of the FEM analysis have been given in Table 1. The dimensions of the core, PCB, winding and insulator layers used for designing geometry of the PT are as given in Table 2. The geometry of the various components of the PT structure were constructed in given dimensions in the geometry building section of the FEM software, with separate coordinate axes for the two slots for window areas of the transformer. Then, after performing several Boolean operations like Boolean subtraction, Boolean Assembly etc., various volumes of the geometry were defined. Finally, a parallelopiped structure was defined around the geometry to act as the infinite box, to specify the domain limits of finite element modelling.

The meshing of this PT structure was done as shown in Fig. 3. Automatic meshing method was employed for calculation and analysis at each node of the mesh. Physical modelling of the PT was performed by implementing a steady state AC Magnetic 3D application. Various materials were assigned for the different regions of the PT by importing them from the software-Material Manager 1.2. Lastly, required non-meshed coils were designed for the primary and secondary coils to carry the currents. Other design parameters of the PT are given in Table 3.

Table 1 Specifications of FEM analysis

Specification	Description
Software	ALTAIR Flux 2020.1
Application	Steady State AC Magnetic 3D
Mesh order	First order
Number of nodes	1074
Number of line elements	782
Number of surface elements	2230
Number of volume elements	4617
Boundary technique	Infinite box (Parallelepiped)

Table 2 Dimensions of components of the PT (in mm)

Component	Dimensions (length × breadth × height)
Core	20.32 × 31.75 × 12.34
PCB layer	24.52 × 25.07 × 1.6
Primary winding layer	24.52 × 25.07 × 0.035
Secondary winding layer	24.52 × 25.07 × 0.035
Insulator layer	24.52 × 25.07 × 0.5

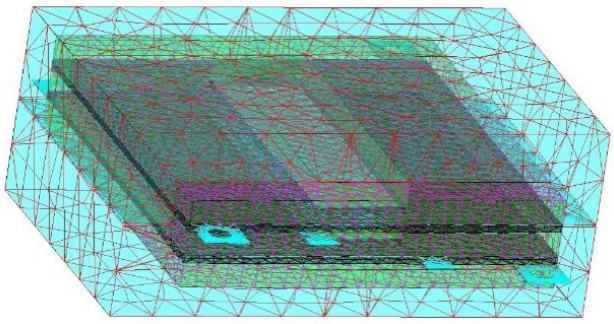

Fig. 3 Meshing diagram of PT

3 Various core and winding materials used for the analysis

3.1 Core materials

In this work, working of the PT has been analyzed with three different core materials, namely: ferrite material, amorphous material, and nanocrystalline material.

3.1.1 Ferrite material

Soft ferrites, which are basically homogenous oxides, are more commonly used for applications like in transformers and inductors, as they deliver a large response even to a "soft" magnetization applied to a small field [18]. These ferrites became a necessity with the advent of higher frequencies, in order to keep the iron losses of devices in check. Typical ferrites belong in either of the two categories – Manganese-Zinc (Mn-Zn) or Nickel-Zinc (Ni-Zn) composition. The properties of these two categories complement each other, thereby extending ferrite application range from as low as a few audio frequencies to as high as several hundred megahertz. The basic complementary properties of Mn-Zn and Ni-Zn is that Mn-Zn has a higher permeability, whereas Ni-Zn has a higher resistivity. Thus, Ni-Zn ferrite is used for frequencies above 1–2 MHz because of its higher resistivity, and Mn-Zn ferrite is used for frequencies less than 2 MHz. Majority of conventional applications require higher permeability at frequencies less than 1 MHz, making Mn-Zn ferrite more commonly used than Ni-Zn. In this work, a Mn-Zn ferrite was used whose properties are listed in Table 3 [18].

3.1.2 Amorphous material

Amorphous material, also called "metallic glass", is basically a solid glassy alloy, which has a disordered atomic-scale

Table 3 Design specifications of the PT

Parameter	Value
Input voltage	100 V
Load rating	2 kW, 50 Ω
Frequency	100 kHz
Turns ratio	2:3
PCB material	Polyamide
Insulator material	Porcelain

structure unlike standard crystalline magnetic materials. They are manufactured by rapid cooling of the melt in such a way that the atoms do not have sufficient time to rearrange into their stable form, and instead forms a metastable structure. But, despite this absence of a long-range structural order of atoms, amorphous materials have similar, and sometimes even lesser densities than that of typical crystalline materials of same composition. They also have the additional advantage of very low core losses, due to their thin foil-like structure, higher permeability, higher induction and higher electrical resistivity [18]. Thus, for high frequency applications, these materials are more preferred than the conventional ferrites, as reducing core losses is very significant at higher frequencies. Also, amorphous materials are more preferred for applications requiring higher saturation flux densities, since they have flux densities of more than 1.5 T, whereas the conventional ferrites have saturation flux density values of about 0.3–0.5 T [4].

Currently available amorphous materials are of three types: Ni-based, Co-based and Fe-based [19]. Ni-based amorphous materials are mostly used for extremely high frequency applications like those above 1 MHz. This is because they exhibit very low core loss value even at such high frequencies. But their low saturation flux density values (around 0.4 T) make them inappropriate for a majority of applications. Co-based amorphous materials also exhibit excellent properties of reduced core loss with moderate saturation flux density values (around 0.7 T) at higher frequencies. But expensive cobalt content usage makes them economically infeasible. Fe-based amorphous materials are widely used for high frequency applications due to their excellent saturation flux density values (around 1.5 T) with a low core loss. They are also advantageous in terms of ease of availability and economic feasibility of iron. In this work, an Fe-based amorphous material has been used, whose properties are listed in Table 3 [19].

3.1.3 Nanocrystalline material

Nanocrystalline materials are also devised to obtain excellent soft magnetic properties than ferrite materials, by employing similar rapid quenching technique as that of amorphous materials. The cooling of the melt is done at about a million degrees per second, to obtain small and uniform "nano-order" crystal grains (about 10 nanometers in size) with even superior soft magnetic properties than amorphous materials. They have even lower core losses than amorphous materials at high frequencies with high saturation flux density values. The only demerit of nanocrystalline materials is their difficult and expensive manufacturing process [19]. The properties of the nanocrystalline materials used in this work is given in Table 4 [18].

3.2 Winding materials

3.2.1 Copper

Copper is the age-old material in use for electrical windings, because of its high conductivity, thereby resulting in less heat losses in electrical machines. Copper also has a very high current-carrying capability, along with other advantageous properties like high ductility and corrosion-resistance. One major disadvantage with copper is its high density, making copper windings, and thereby electrical machines more heavier. Some of the important parameters of copper windings implemented is given in Table 5 [18].

3.2.2 Aluminum

Aluminum is also in use as electrical winding material due to its lesser cost and weight than copper windings. Aluminum is less dense, and has a higher heat capacity than copper, giving it the ability to withstand higher current overloads. But its conductivity is lesser than copper, and hence larger amount of windings is required for the same output, thereby simultaneously increasing the losses of the machine. Thus, aluminum windings are considered mostly when weight and heat capacity is important as in the case of high frequency applications. Main properties of aluminum windings used for analysis is given in Table 5 [18].

Table 4 Properties of core materials used

Property	Ferrite core	Amorphous core	Nanocrystalline core
Material name	Mn-Zn	Metglas 2605SC	Vitroperm 500F
Initial relative permeability	5000	1500	30000
Saturation flux density (T)	0.43	1.56	1.24
Curie temperature (°C)	145	370	460
Resistivity (Ωm)	0.5	1.3	1.15
Density (kg/m^3)	4800	7180	7350

Table 5 Properties of winding materials used

Material	Resistivity ρ (in Ωm)	Temperature coefficient of resistance α (in K^{-1})	Density (in kg/m^3)
Cu	1.56×10^{-8}	3.9×10^{-3}	8960
Al	2.65×10^{-8}	3.8×10^{-3}	2710
CNT	1×10^{-8}	-0.2×10^{-3}	1000
Cu/CNT	2.2×10^{-8}	-4×10^{-4}	3000
Al/CNT	2.96×10^{-8}	-2×10^{-4}	2000

3.2.3 CNT

CNTs are basically allotropes of carbon, currently being used to replace heavier winding materials like copper in electrical machines. They have extremely low densities with a maximum of about 1000 kg/m^3, which is almost one-eighth of that of copper, and half of that of aluminum. Thus, size and weight of electrical machines can be significantly reduced on using CNT windings. They have very good conductivity values also, due to their one-dimensional and symmetrical structure of atoms. Even though conductivity of pure metal conductors has not yet been matched with CNT windings, conductivities almost close to Al has been recently achieved today with CNT. Thus, CNTs prove to be an excellent replacement for metals like copper and aluminum, which are difficult to extract from ores and expensive too, owing to their huge demand in a majority of developing nations. The properties of the CNT windings used in this analysis are given in Table 5 [20, 21].

3.2.4 Cu/CNT

Cu/CNT is a CNT composite made by merging copper with CNT to enhance its electrical, thermal and mechanical properties. These Cu/CNT composites depicts superior conductivity values than individual CNT fibers, because of its collaboration of metallic properties of copper [22]. It also incorporates the light-weight nature of carbon, thereby reducing the density and weight of the machine significantly, when compared to pure copper winding usage. The properties of Cu/CNT composite windings used in this analysis is given in Table 5 [20, 21].

3.2.5 Al/CNT

Al/CNT is also another newly explored prospective CNT composite aimed to replace conventional electrical windings [23]. Aluminum is more advantageous than copper on account of its light-weight and cheapness. But conductivity of aluminum is not high enough to match the more promising Cu/CNT composite, especially in applications demanding high electrical conductivity. The properties of Al/CNT composite windings used for this analysis is given in Table 5 [20, 21].

4 Estimation of core losses of the PT with various materials

Core losses are inevitable in devices like transformers and inductors involving a magnetic core. When the magnetic core of these devices is subjected to a changing current, some part of the power to be ideally transmitted through the device gets lost as heat. This basically comprises the core losses of the device.

Manufacturers now present core loss (P_{core}) in Eq. (1) giving the losses in W/kg [18]:

$$P_{\text{core}} = k \times f^m \times B^n , \tag{1}$$

where f is the frequency of operation and B is the magnetic flux density value. The coefficients k, m and n provided by manufacturers, vary based on several factors such as the frequency range of operation, type and size of material used etc. These coefficients of all the three core materials analyzed are given in Table 6 [18]. FEM was used to determine the magnetic flux density values of the PT with all combinations of core and winding materials, and the results obtained are given in Table 7.

With these magnetic flux density results and the core loss coefficients given in Table 5, Eq. (1) was evaluated to determine the core loss in W/kg. The final core loss in watts was obtained by determining the weight of the core using density and volume. The analytical core loss values thus obtained are given in Table 8.

From Table 8, it is seen that core losses vary based on the winding materials used, as core loss equation given in Eq. (1) involves magnetic flux density term, whose distribution is influenced by the winding material used. From

Table 6 Core loss coefficients of the core materials used

Coefficient	Ferrite core	Amorphous core	Nanocrystalline core
k	2.4×10^{-4}	10.1×10^{-6}	0.8×10^{-6}
m	1.6	1.5	1.8
n	2.5	1.6	2.1

Table 7 Simulated magnetic flux density values (in Tesla) of the PT

Winding material	Ferrite core	Amorphous core	Nanocrystalline core
Cu	0.433	1.535	1.151
Al	0.480	1.544	1.156
CNT	0.321	1.527	1.146
Cu/CNT	0.300	1.510	1.135
Al/CNT	0.317	1.519	1.141

Table 8 Analytical core loss values (in Watts) of the PT

Winding material	Ferrite core	Amorphous core	Nanocrystalline core
Cu	296.81	115.01	109.63
Al	390.76	116.07	110.63
CNT	141.80	114.04	108.63
Cu/CNT	120.67	112.01	106.45
Al/CNT	130.98	113.08	107.64

the analytical core loss results, it is concluded that nanocrystalline core gives the lowest core losses with all the five different windings analyzed.

FEM results giving the magnetic flux density distributions of ferrite, amorphous and nanocrystalline core are given in Fig. 4. From Fig. 4 (a), it is seen that the magnetic flux density distribution of ferrite core is in such a way that the majority of the core operates at a flux density of around 0.3 T, where the B_{max} value of the ferrite core is 0.43 T (see Table 3). This shows that the transformer design is optimized with the least possible core losses and highest possible magnetic flux density for ferrite. From Fig. 4 (b), it is seen that the major portions of the amorphous core operate at a magnetic flux density value of about 1.3 T, where the B_{max} value of amorphous core is 1.56 T. Similarly, from Fig. 4 (c) also, it is seen that major portions of the core are operating around 1 T, which is close to B_{max} value 1.24 T of nanocrystalline core.

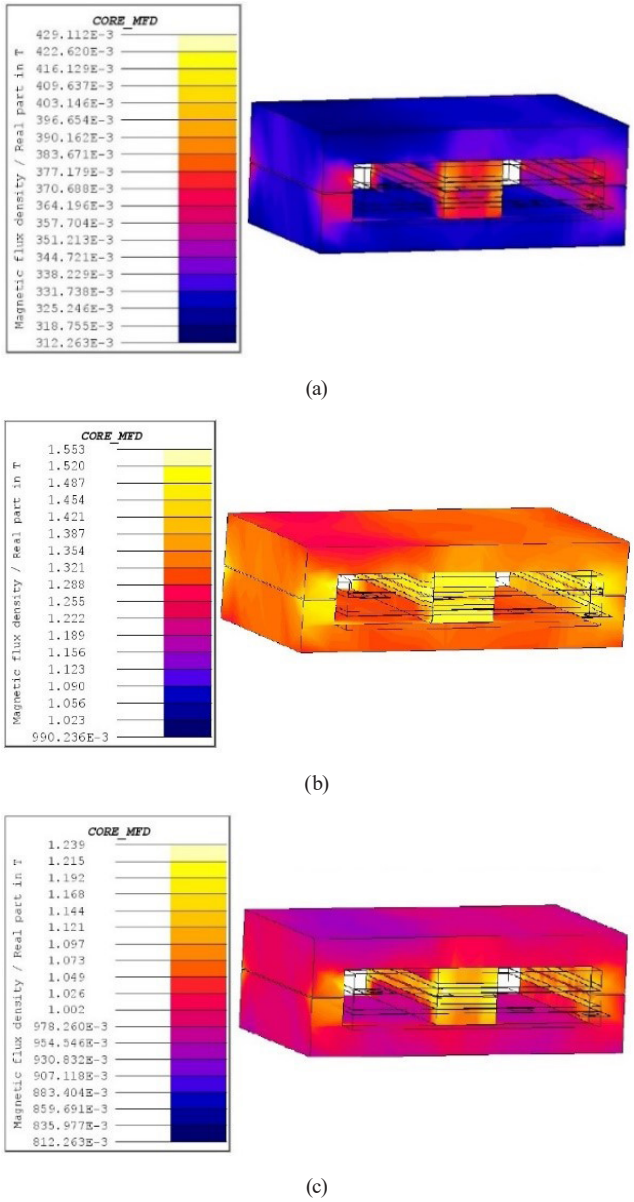

Fig. 4 Magnetic flux density distribution of (a) Ferrite core (b) Amorphous core (c) Nanocrystalline core

To validate the analytical core loss results obtained in Table 8, FEM simulations were done to determine power losses in core in W/m^3. These were multiplied with the volume of the PT core simulated (which was found to be 21.38 cm^3) to obtain the final simulated core loss values in Watts, given in Table 9.

The analytic results of the core loss measurement given in Table 8 have been validated by the FEM measurement results of the core losses of the PT given in Table 9 and is shown in Fig. 5. As seen from the graph, for all the three core materials used, the analytic and measured values of core losses correspond to each other very well, thus validating the FEM methodology used.

The core loss distributions of ferrite, amorphous and nanocrystalline cores are given in Fig. 6. For all the three cores, similar to the magnetic flux density distributions, core loss is also seen to be higher near the transformer window areas where the windings are accommodated. Also, there is a slightly higher concentration of losses around the central air gap region of the core and near the sharp edges of the core, which is as expected for higher surface area regions.

Fig. 7 shows the average reduction in core losses of the PT on using amorphous or nanocrystalline cores instead of the conventional ferrite core. It is found that the core losses are reduced by about 48.14% on using amorphous or nanocrystalline cores.

Table 9 Final simulated core loss values (in Watts) of the PT

Winding material	Ferrite core	Amorphous core	Nanocrystalline core
Cu	288.74	112.50	109.50
Al	389.27	113.57	110.57
CNT	138.81	111.64	108.43
Cu/CNT	118.06	111.86	106.30
Al/CNT	128.11	110.58	107.58

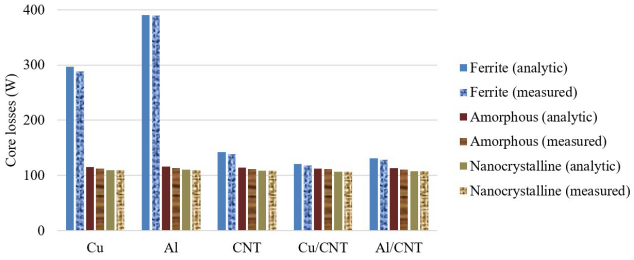

Fig. 5 Comparison of analytical and measured FEM results of core losses

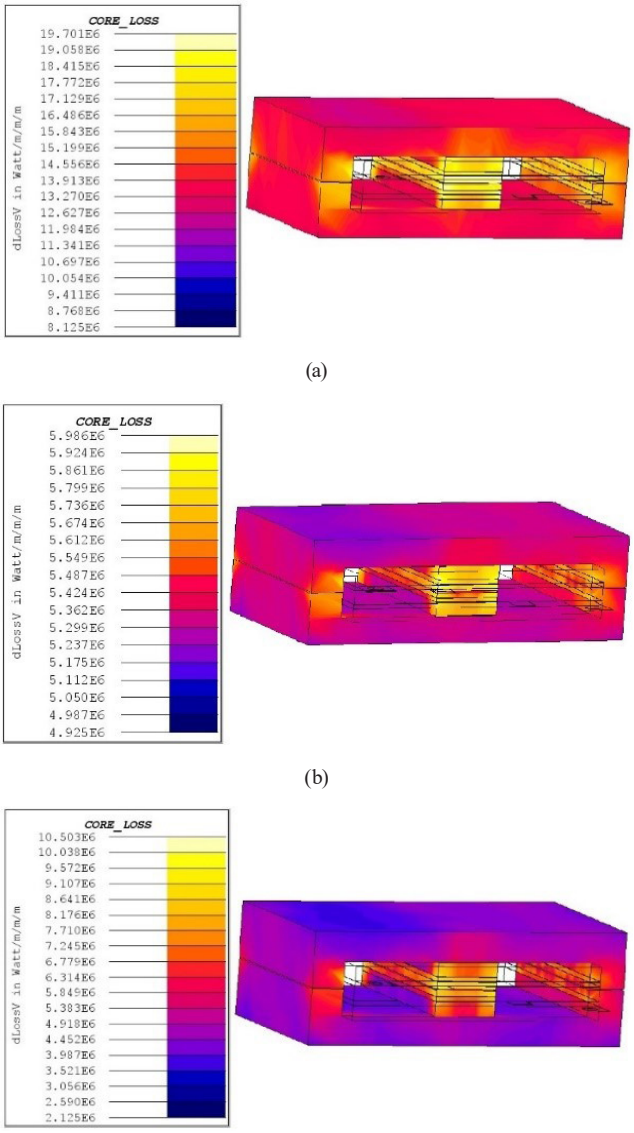

Fig. 6 Core loss distribution of (a) Ferrite core (b) Amorphous core (c) Nanocrystalline core

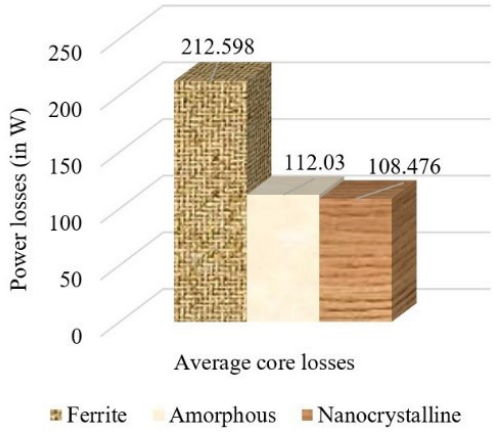

Fig. 7 Comparison of losses of various core materials

5 Estimation of winding losses of the PT with various materials

Winding losses are comparatively smaller in PTs when compared to traditional wire-wound transformers because of the planar windings implemented in the PT. Winding losses are basically I^2R losses, which can be calculated by determining the winding resistance (R) of the windings at working temperature, given by Eq. (2) [24]:

$$R = R_{DC}[1 + \alpha \times \Delta T], \tag{2}$$

where α is the temperature coefficient of resistance, ΔT is the difference between working temperature and default room temperature, and R_{DC} is the winding resistance at default room temperature, given by

$$R_{DC} = \frac{\rho \times l}{A}, \tag{3}$$

where ρ is the resistivity of the winding material (in Ωm), l is the length of the winding (in m) and A is the cross-sectional area of the winding (in m^2).

Therefore, to calculate the analytical values of winding losses in the PT with various windings, all these above-mentioned parameters are defined as given in Table 10 [24].

The ρ and α values of all the five winding materials have been given in Table 4. Length and volume of the winding were found from the geometry design. The winding is cylindrical with its radius of cross-section being 0.125 mm; hence with this, area of cross-section was found. A working temperature of 125 °C was chosen to obtain the winding losses towards the extreme high end of possible temperature range of a medium power PT [25]. With all these values, analytical winding losses of the PT with all the five different materials have been found and are given in Table 11.

From the results of Table 10, it is seen that for the 2-kW PT simulated, winding losses are very less with all the five winding materials analyzed, and among them, CNT

Table 10 Parameters for calculation of winding losses of the PT

Parameter	Value
l (in mm)	352.8
A (in mm^2)	0.049
Current through winding (in A)	26.97
Winding volume (in mm^3)	77.21
Default temperature (in °C)	20
Working temperature (in °C)	125

Table 11 Analytical winding losses (in Watts) of the PT with various materials

Material	Winding loss
Cu	8.898
Al	14.959
CNT	3.951
Cu/CNT	8.507
Al/CNT	11.712

windings are giving the lowest losses. FEM simulations were done on the PT to determine winding power losses in W/m^3. These were multiplied with the volume of the windings simulated to obtain the final simulated winding loss values in Watts, which is given in Table 12.

From Table 12, it is seen that the simulated winding losses validate the analytically obtained winding losses given in Table 11. Cu/CNT windings are observed to result in an almost same amount of losses as that of pure Cu windings, along with the additional advantage of light-weight nature of windings due to CNT integration. Pure Al windings results in the highest losses having lower conductivity than copper, but with Al/CNT composite windings, losses are slightly reduced. CNT windings give the lowest losses along with the advantage of low weight.

The winding losses of all the five winding materials are given in Fig. 8. The simulations show that the losses are higher along the path of the winding arrangement as expected, according to the winding placement shown in Fig. 2. Also, there is a concentration of losses towards the front and rear sides of the winding arrangement, and also around the terminals of both the primary and secondary windings, due to decreased surface regions of the winding placement.

Fig. 9 shows the average reduction in winding losses of the PT on using the five different winding materials. It is found that the winding losses are reduced by about 56.2% on using CNT windings instead of conventional copper windings.

Table 12 Final simulated winding loss values (in Watts) of the PT

Winding material	Ferrite core	Amorphous core	Nanocrystalline core
Cu	8.897	8.733	8.563
Al	14.958	14.757	14.613
CNT	3.950	3.839	3.683
Cu/CNT	8.506	8.386	8.224
Al/CNT	11.711	11.439	11.282

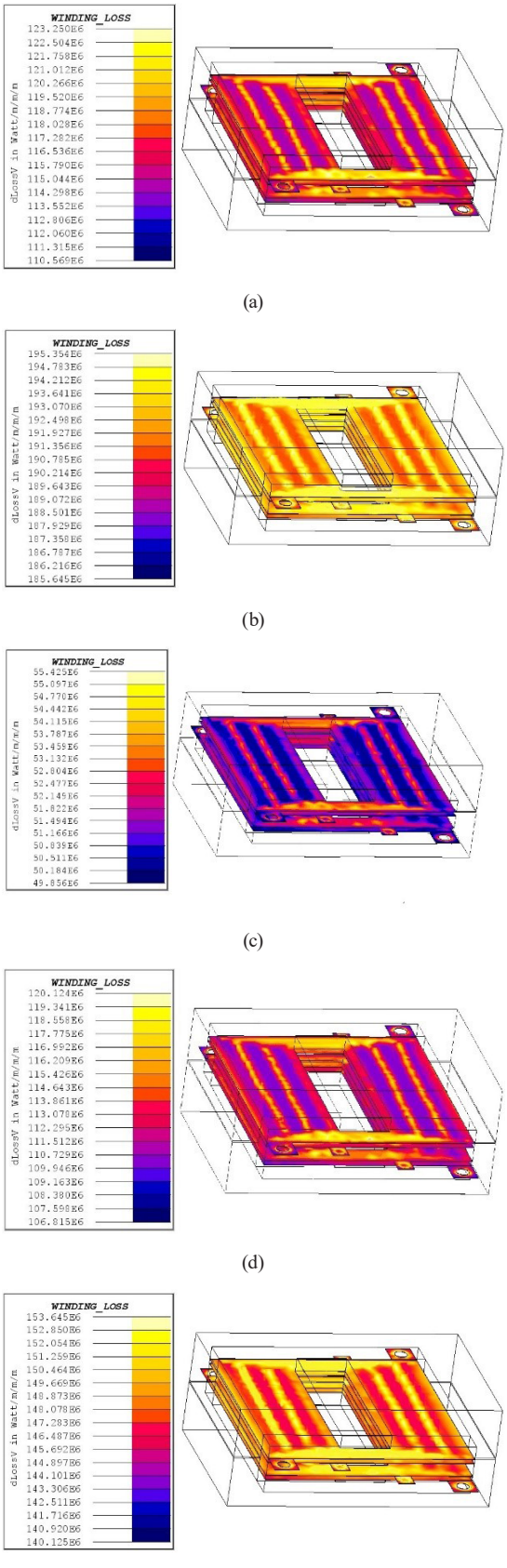

Fig. 8 Winding losses distribution of (a) Cu (b) Al (c) CNT (d) Cu/CNT (e) Al/CNT

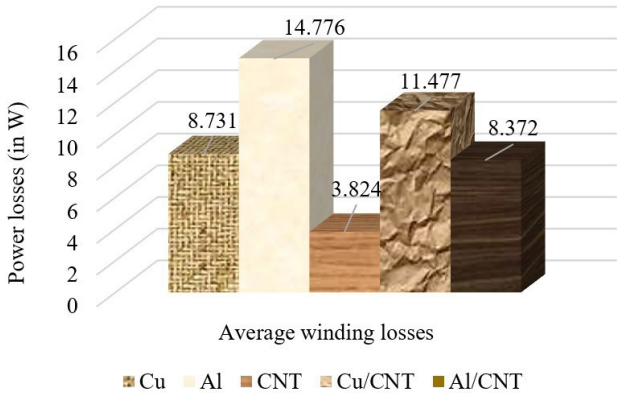

Fig. 9 Comparison of losses of various winding materials

6 Conclusion

This work was focused on the effect of various emerging core and winding materials on the losses of a high frequency, medium power PT. From the analysis of core losses using FEM, it was observed that emerging core materials such as amorphous and nanocrystalline materials reduced the core losses of the PT by about 48.14% when compared to traditional ferrite core losses. Winding losses were reduced by around 56.2% on using CNT windings, instead of conventional copper windings. Composite materials like Cu/CNT and Al/CNT also resulted in lower losses than their pure metal forms. Also, it was observed that variation in winding materials varied the core losses, even though slightly, since core loss calculation included magnetic flux density analysis, which varied with the winding material used. However, variation in core materials had little to no effect on the winding losses. The best combination of core and winding material that resulted in the lowest possible core and winding losses was nanocrystalline material with CNT windings.

Acknowledgement

This work is part of SRMIST Selective Excellence Research Initiative-2021: "DCFCEVB".

References

[1] Battal, F., Balci, S., Sefa, I. "Power electronic transformers: A review", Measurement, 171, 108848, 2021. https://doi.org/10.1016/j.measurement.2020.108848

[2] Mishra, D. K., Ghadi, M. J., Li, L., Hossain, M. J., Zhang, J., Ray, P. K., Mohanty, A. "A review on solid-state transformer: A breakthrough technology for future smart distribution grids", International Journal of Electrical Power & Energy Systems, 133, 107255, 2021. https://doi.org/10.1016/j.ijepes.2021.107255

[3] Li, L., Du, X., Pan, J., Keating, A., Matthews, D., Huang, H., Zheng, J. "Distributed magnetic flux density on the cross-section of a transformer core", Electronics, 8(3), 297, 2019. https://doi.org/10.3390/electronics8030297

[4] Rodriguez-Sotelo, D., Rodriguez-Licea, M. A., Araujo-Vargas, I., Prado-Olivarez, J., Barranco-Gutiérrez, A.-I., Perez-Pinal, F. J. "Power Losses Models for Magnetic Cores: A Review", Micromachines, 13(3), 418, 2022. https://doi.org/10.3390/mi13030418

[5] Vibhuti, Walia, G., Bhalla, D. "Assessment of the use of FEM for computation of Electromagnetic Forces, Losses and Design of Transformers", Journal of Physics: Conference Series, 1478, 012029, 2020. https://doi.org/10.1088/1742-6596/1478/1/012029

[6] Theisen, E. A. "Recent Advances and Remaining Challenges in Manufacturing of Amorphous and Nanocrystalline Alloys", IEEE Transactions on Magnetics, 58(8), 2001207, 2022. https://doi.org/10.1109/TMAG.2022.3163713

[7] Azuma, D., Ito, N., Ohta, M. "Recent progress in Fe-based amorphous and nanocrystalline soft magnetic materials", Journal of Magnetism and Magnetic Materials, 501, 166373, 2020. https://doi.org/10.1016/j.jmmm.2019.166373

[8] Zhang, X., Lin, H., Shang, H., Xu, J., Zhu, J., Huang, W. "Recent advances in functional fiber electronics", SusMat, 1(1), pp. 105–126, 2021. https://doi.org/10.1002/sus2.1

[9] Dariyal, P., Arya, A. K., Singh, B. P., Dhakate, S. R. "A review on conducting carbon nanotube fibers spun via direct spinning technique", Journal of Materials Science, 56(2), pp. 1087–1115, 2021. https://doi.org/10.1007/s10853-020-05304-z

[10] Robert, F., Prince, A. A., Fredo, A. R. J. "Investigation of using CNT and Cu/CNT Wires for Replacing Cu for Power Electronics and Electrical Applications", ECS Journal of Solid State Science and Technology, 11(2), 023011, 2022. https://doi.org/10.1149/2162-8777/ac5471

[11] Mohd Nurazzi, N., Asyraf, M. R. M., Khalina, A., Abdullah, N., Sabaruddin, F. A., Kamarudin, S. H., …, Sapuan, S. M. "Fabrication, functionalization, and application of carbon nanotube-reinforced polymer composite: An overview", Polymers, 13(7), 1047, 2021. https://doi.org/10.3390/polym13071047

[12] Robert, F. "Power withstanding capability and transient temperature of carbon nanotube-based nano electrical interconnects", ECS Journal of Solid State Science and Technology, 10(6), 061008, 2021. https://doi.org/10.1149/2162-8777/ac07fb

[13] Talaat, A., Suraj, M. V., Byerly, K., Wang, A., Wang, Y., Lee, J. K., Ohodnicki Jr, P. R. "Review on soft magnetic metal and inorganic oxide nanocomposites for power applications", Journal of Alloys and Compounds, 870, 159500, 2021. https://doi.org/10.1016/j.jallcom.2021.159500

[14] Natarajan, B. "Processing-structure-mechanical property relationships in direct formed carbon nanotube articles and their composites: A review", Composites Science and Technology, 225, 109501, 2022. https://doi.org/10.1016/j.compscitech.2022.109501

[15] Orosz, T. "Evolution and Modern Approaches of the Power Transformer Cost Optimization Methods", Periodica Polytechnica Electrical Engineering and Computer Science, 63(1), pp. 37–50, 2019.
https://doi.org/10.3311/PPee.13000

[16] Shafaei, R., Perez, M. C. G., Ordonez, M. "Planar Transformers in LLC Resonant Converters: High-Frequency Fringing Losses Modeling", IEEE Transactions on Power Electronics, 35(9), pp. 9634–9651, 2020.
https://doi.org/10.1109/TPEL.2020.2971424

[17] Venugopal, A., Robert, F. "Analysis of a Non-overlapping Interleaved Planar Transformer Winding Structure with Reduced Parasitic Effects", Iranian Journal of Science and Technology, Transactions of Electrical Engineering, 46(3), pp. 689–700, 2022.
https://doi.org/10.1007/s40998-022-00507-3

[18] McLyman, C. W. T. "Transformer and Inductor Design Handbook" 4th ed., Taylor & Francis, 2017. ISBN 9781138198258

[19] Sarker, P. C., Islam, M. R., Guo, Y., Zhu, J., Lu, H. Y. "State-of-the-Art Technologies for Development of High Frequency Transformers with Advanced Magnetic Materials", IEEE Transactions on Applied Superconductivity, 29(2), 7000111, 2019.
https://doi.org/10.1109/TASC.2018.2882411

[20] Lekawa-Raus, A., Patmore, J., Kurzepa, L., Bulmer, J., Koziol, K. "Electrical Properties of Carbon Nanotube Based Fibers and Their Future Use in Electrical Wiring", Advanced Functional Materials, 24(24), pp. 3661–3682, 2014.
https://doi.org/10.1002/adfm.201303716

[21] Chengdu Organic Chemicals Co. Ltd., Chinese Academy of Sciences "Carbon Nanotube Fibers Composite Wires", [online] Available at: http://www.timesnano.com/en/view.php?prt=3,35,158,188 [Accessed: 03 December 2021]

[22] Sundaram, R. M., Sekiguchi, A., Sekiya, M., Yamada, T., Hata, K. "Copper/carbon nanotube composites: research trends and outlook", Royal Society Open Science, 5(11), 180814, 2018.
https://doi.org/10.1098/rsos.180814

[23] Mohammed, S. M. A. K., Chen, D. L. "Carbon Nanotube-Reinforced Aluminum Matrix Composites", Advanced Engineering Materials, 22(4), 1901176, 2020.
https://doi.org/10.1002/adem.201901176

[24] Marchio, S. "Designing With the PLA51 Planar Transformer for Enhanced Power Density and Efficiency", Transformers: Application Note, Vishay Sfernice Ltd., 59063, 2017.

[25] Vishay Electronics, "Medium Power Planar Transformer 1 kW to 3 kW", [pdf] PLA51, Vishay Sfernice Ltd., 59059, 2016. Available at: http://www.farnell.com/datasheets/2245234.pdf [Accessed: 03 December 2021]